Journal of the Korean Physical Society, Vol. 47, No. 5, November 2005, pp. 764∼776

Simple Modeling of Stochastic Classical Nano-Bit Data Corruption: Probability Distribution Consideration

Suchittra Sa-Nguansin
Department of Mathematics, Faculty of Science, Mahidol University, Bangkok, Thailand Department of Mathematics, Faculty of Science, Naresuan University, Pitsanulok, Thailand, Bangkok

Wannapong Triampo* and Narin Nattavut
Department of Physics, Faculty of Science, Mahidol University, Bangkok, Thailand Capability-building Unit in Nanoscience and Nanotechnology, Faculty of Science, Mahidol University, Thailand, Bangkok

(Received 29 March 2005, in final form 8 July 2005)

Motivated by a real-world application of quantum-dot cellular automata (QCA) and with the help of Monte-Carlo simulations and analytic continuum theory, we have studied the corruption or error process of a binary nano-bit model resulting from an interaction with stochastically independent Brownian agents (BAs). Besides, the more specific link to a real-world application, in this work, we have extended the scope of the study and have used the new technique to reproduce results from previous works by Newman and Triampo [Phys. Rev. E **59**, 5172 (1999) and Phys. Rev. E **60**, 1450 (1999)]. The new findings include 1) the effect of a "patch" or "cluster" of bits on the simulation results, 2) the log-normal vs. normal distribution of the local bit density, and 3) new results for local bit corruption in two dimensions. The theory is compared with the results of simulations, and good agreement is found. The connection of this binary nano-bit model with the real world is discussed, especially in the context of molecular electronics and the quantum-dot cellular automata paradigm. With model extension such as taking into account a more realistic correlation between bits, our hope is that this work may contribute to an understanding of the soft error or the corruption of data stored in nano-scale devices.

PACS numbers: 05.20.-y
Keywords: Molecular bit, Brownian agent, Data bit corruption, Binary system, Probability distribution

I. INTRODUCTION

With the advent of nanotechnology, the use of properties and phenomena of physical and biological systems occurring on a nanoscale has rapidly revolutionized many areas of interdisciplinary research, such as nanomedicine [1–4], nanobiotechnology [5, 6] and nanoelectromechanical systems [3–5, 7]. In the field of microelectronics, the trend towards higher speeds and greater packing densities requires scaling to smaller lithographic dimensions. The nanotechnolgy revolution is having a strong impact on nanoelectronics and molecular computing and is leading to the replacement of conventional scaling of Si CMOS electronic devices with single-electron transistors (SETs) or carbon-based nanoelectronic devices. This has made electronic components ever smaller with as a high a capacity as possible with less power consumption [8–10]. To decrease the number of electrons used to switch MOS transistors on a chip, the circuits are designed to operate as binary logic gates in which a binary state is characterized by the absence or presence of a single electron or a few electrons in isolated islands. However, when this kind of CMOS-like chip is fabricated with the number of electrons becoming ultra small (less than 1000), one usually experiences the problem of statistical variations in the sub-threshold characteristics due to stochastic single-electron tunneling causing charge fluctuations. In dynamic random access memories (DRAMs), for another example, the number of charges stored per memory cell has been decreased with the reduction of the cell area. However, when the stored charges per bit are further decreased, the signal becomes "less immune" to internal noise, the leakage current, and soft errors caused by the passage of ionizing radiation. This will interfere with the charge held at sensitive nodes in the circuits [11]. Therefore, for the present semiconductor industry to produce ever-smaller memory devices, properties such as the reliability, volatility, and power consumption must

*E-mail: wtriampo@yahoo.com

be of concern. As the data storage density has been increased, data fidelity is subject to random noise so the reliability or stability of a device must be considered as a stochastic nano-bit error or as nano-bit data corruption. One may consider ultra small bit systems as binary bit systems consisting of bits "1" or "uncorrupted bits" and bits "0" or "soft-error or corrupted bits" The dynamics of error causing or corruption is incorporated using simple Brownian agents and even other various kinds of agents.

In the present work, we adopt the model introduced by Newman and Triampo [12,13] and recast it into the nano-bit context. The model consists of Brownian agents (BAs) stochastically corrupting their nano-bit (ultra-small binary bit) environment. The corrupting agents perform random walk motion and are not affected by their environment in any way (no landscape-feedback). As the agents wander through the environment, they have a certain probability to switch the value of the nanobit at the site as they are leaving. One can also consider the agents to be disordering agents in their environment. Rationalization and the connection to real-world applications is considered in the next section. In the near future, however when ever-smaller (nano-bit) devices become more widespread, our study might be of importance for stochastic soft-error process. The focus of this study is the time and the length scales of corruption due to independent BAs.

The paper is organized as follows: in Section II, we give the details of the model, focusing on the local nano-bit corrupting parameter at the origin, $b(0,t)$ and its associated probability distribution $P(b,0,t)$. In Section III, we show some numerical results. We then summarize our results and make some comments in Section IV.

II. RATIONALIZATION OF THE MODEL AND A CONNECTION TO A REAL-WORLD APPLICATION: MOLECULAR ELECTRONICS

In the past decades, there has been a nearly exponential growth in the capacities of silicon-based microelectronics [14]. According to the famous rule of thumb proposed by Gordon Moor, co-founder of the chip manufacturer Intel, which states that, the number of transistors that can be packed onto a microprocessor doubles every 1.5 or 2 years, however, it is believed that conventional silicon-base computers will reach their physical limits around 2012, mainly because of fundamental physical limitations that prevent current designs from functioning reliably on a nanometer scale such as the insurmountable current leakage problem of transistors. Thus there is an urgent realization that silicon-based microelectronics are heading toward a wall. In this regard, the challenge ahead is to find an alternative electronic paradigm to silicon-based chips that will allow the rise in computational power to continue (maybe slower or faster). Molecular electronics [15] can, in principle, overcome these limitations of silicon-based technology because single-molecule devices that are organized cheaply in parallel by using self-assembly are possible. This is a powerful new direction in the science and technology of nanometer-scale devices. Simple molecular electronic devices usually consist of organic molecules sandwiched between conducting electrodes, with recent demonstrations of irreversible switches [16], large negative differential resistances [17] and quantum-dot cellular automata [18–21]. However, reaching agreement between experiments and theory has not been straightforward. Especially, an understanding of the molecule/electrode interface is very crucial. So far, the field of molecular electronics is teeming with results, rationalizations, and speculations. The developments of the past few years have convinced some within the computer industry that molecular electronics will eventually deliver the goods. We believe that the next-generation technologies will most likely consist of hybrid devices combining molecular electronics and existing microelectronics.

At present, a conventional computer utilizes microprocessors, silicon field-effect transistors (FETs). These have three terminals: the source (input), the drain (output) and the gate (control). They operate by using binary "0" and "1" bits as the "on" and the "off" states of a current switch to store and process information. This all happens in the hardware called a transistor. The transistor acts as a current switch to charge and discharge capacitors to the required logic voltage levels. This conventional FET paradigm has serious drawbacks as device sizes are reduced. As the switch get smaller (about 1.5 nm), the ability and the reliability to turn the current on and off is lower. Moreover, when the switch is smaller in size, the current feeding through each switch is reduced, subsequently causing the power supply to feed the energy to move the electron (by passing an electric current through the circuit). This is likely to cause significant energy dissipation that could generate a lot of heat. This unwanted heat could damage, even melt, thermally organic materials. This evidence indicates that to ultimately reduce the size of electronic devices, a new paradigm must be developed to take care of all the down sides. An alternative approach will be discussed in the following.

The quantum-dot cellular automata (QCA) are the alternative nanostructure-compatible computational paradigm using arrays of quantum-dot cells ("QCA cells") to implement a digital logic function. This scheme is fundamentally based on the Coulomb interactions occurring between neighboring cells where each cell can be a single molecule. Unlike FETs, which use current and voltage to encode binary information, QCAs instead use the arrangement of individual electrons by positioning of interacting single electrons within arrays of quantum dots to represent binary information. This system is a type of transistorless nanoelectronic device represented by a structured charge container. In this paradigm, each

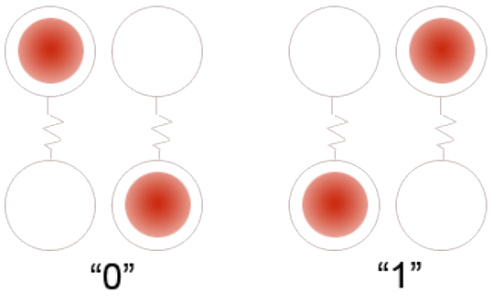

Fig. 1. A schematic of a QCA cell or a two-state four-dot cell. Due to Coulomb repulsion, the electrons, shown in red, normally occupy antipodal sites. A "0" or "1" bit is encoded in the charge configuration. It should be noted that the full four-dot cell can be viewed as a pair of half-cells with two dots each, in which the sign of the dipole alternates.

QCA cell consists of four dots or clusters localized at the corners, or the so-called vertices, of a square. A dot for this purpose is a region in which charge is localized. When two excess electrons are added to the cell (by charging), due to mutual electrostatic repulsive forces, they will arrange themselves by occupying diagonal sites so as to keep as far a part as possible. Hence, there are two diagonal polarizations of energetically equivalent bistable ground states of the cell (degeneracy); if they were compass points, one would lie NW-SE and the other NE-SW, which are used to represent logic "0" and logic "1" (see Fig. 1). When, for example, an electric field is applied, the electrons will switch sites in one set of dots, thus inducing the switch in an adjacent set of dots to change the polarization in a QCA cell. Experimentally, the operation of a QCA can be demonstrated by constructing micrometer-sized clusters of atoms, such as aluminium "islands", which can be described as "quantum dot" and can store electrons. These can, for example, be assembled on an oxidized silicon surface.

With this ultrasensitive nano-switch, we expect this nano-bit system to be vulnerable to "fluctuations" or "disturbances". This is typically caused by noise, any unwanted or obscuring signal. The noise behavior of bulk electronic devices is dominated primarily by two noise sources: thermal noise and Ficker (1/f) noise. Other sources that are sometimes present in the noise spectrum are shot noise. Using magnetic spin language, the phenomenon involves generating noise which includes thermal spin fluctuations and magnetic domain instabilities (magnetization orientation fluctuation). Noise is universally encountered in semiconductors, and in many cases, the performances of semiconductor devices are limited. Noise in semiconductor devices refers to any unwanted signal or disturbance in the device that degrades performance. Shrinking device size implies increasing noise and faster noise. This effect, the stronger and faster noise and the shrinking noise margin, synergistically increase the frequency of false bit flips when miniaturization approaches a critical size. A detailed knowledge of the charge transport processes leading to electronics noise and of the microscopic states involved in these processes is necessary to reduce the noise and to improve device performance. This is, in fact, the issue of stability and reliability of electronic devices. In this regards, we shall treat fluctuators as stochastic agents, such as thermal fluctuators and photons that consistently and continuously change the nano-bits in this system. It should be pointed out with no confusion that on the scale of an individual molecule, quantum effects might also limit reliability. In theory, molecular switches can operate incredibly quickly, with switching times measured in femtoseconds rather than the nanosceconds of today's silicon FETs, the uncertainty principle will limit the precision with which the states of switches can be measured, and thus the feasibility of storing and processing information. However, the agents, as mentioned, may cause an issue with the stability and the reliability of this sensitive system.

III. NANO-BIT CORRUPTION MODEL (REVISITED)

In this section, we revisit the related theoretical results in Refs. 12 and 13 for the reader to understand investigations of data corruption through simulations. For the sake of simplicity, we begin with a model consisting of just one agent. The process of a stochastic agent in a nano-bit medium is first modeled on a hypercubic lattice of dimension $d = 1$. In the spirit of the local rules using a stochastic cellular automaton (SCA) [22], the process is then defined in terms of the position $\vec{R}(t)$ of the BA. At each time step, the BA makes a random jump to one of its nearest neighbors. The spin at the site it leaves behind is flipped. To make the discussion more familiar, we will represent the stochastic binary system as an Ising model consisting of bits "1" or uncorrupted bits, and "−1", or corrupted bits. We denote a randomly chosen unit vector as $\vec{l}(t)$ and the time -dependent value of the spin at site $\vec{r}$ as $\sigma_{\vec{r}}(t)$. Then, we have

$$\vec{R}(t+\delta t) = \vec{R}(t) + \vec{l}(t) \quad (1)$$

and

$$\sigma_{\vec{r}}(t+\delta t) = \sigma_{\vec{r}}(t)(1 - 2\delta_{\vec{r},\vec{R}(t)}). \quad (2)$$

Equation (2) is taken in the continuum limit viewing the discrete spins as a coarse-grained local spin bit corruption density $\phi(\vec{r}, t)$. In other words, we are defining a large region around the lattice site $\vec{r}$ and summing all the spins in that region. The evolution of the bit corruption density ϕ is then described by

$$\partial_t \phi(\vec{r}, t) = -\lambda \phi(\vec{r}, t) \delta^d(\vec{r} - \vec{R}(t)), \quad (3)$$

where λ is a phenomenological parameter that describes how strongly the spin is coupled to the BA. This equation may be integrated to give the explicit functional solution

$$\phi(\vec{r},t) = \exp[-\lambda \int_0^t dt' \delta^d(\vec{r} - \vec{R}(t'))]. \quad (4)$$

The above solution is obtained for an initial condition $\phi(\vec{r},0) = 1$ (completely uncorrupted), which we shall use exclusively.

For the sake of analytic simplicity, we will from now on focus only on the one dimension case, $d = 1$. The simplest quantity to be considered is the mean bit corruption density defined as

$$b(\vec{r},t) = \langle \phi(\vec{r},t) \rangle = \Sigma_{n=0}^{\infty} (-\lambda)^n \chi_n(x,t), \quad (5)$$

where $\chi_0(x,t) = 1$, and for $n > 0$,

$$\chi_n(x,t) = \frac{1}{n!} \left\langle \left[\int_0^t d\tau \delta(x - R(\tau)) \right]^n \right\rangle. \quad (6)$$

Further details and discussion can be found in Ref. 12. With the average over the Gaussian weight, it can be shown that

$$\chi_n(x,t) = \int_0^t d\tau_1 \int_0^{\tau_1} d\tau_2 \cdots \int_0^{\tau_{n-1}} d\tau_n g(0, \tau_1 - \tau_2) \cdots \times g(0, \tau_{n-1} - \tau_n) g(x, \tau_n), \quad (7)$$

where $g(x,t) = (2\pi Dt)^{-1/2} \exp(-x^2/2Dt)$ is the probability density of the random walk and D is the diffusion constant. Due to the structure of Eq. (7), which is an n-fold convolution, we can apply a temporal Laplace transform and have (for $n > 0$)

$$\tilde{\chi}_n(x,s) \equiv \int_0^{\infty} dt e^{-st} \chi_n(x,t) = \frac{1}{s} \tilde{g}(0,s)^{n-1} \tilde{g}(x,s), \quad (8)$$

where

$$\tilde{g}(x,s) = \frac{1}{(2Ds)^{1/2}} \exp\left[- \left(\frac{2s}{D} \right)^{1/2} |x| \right], \quad (9)$$

with $\tilde{g}(x,s)$ being the Laplace transform of the diffusion equation Green's function.

Summing over these functions as formulated in Eq. (5), we find

$$\tilde{b}(x,s) = \frac{1}{s} \exp\left[1 - \frac{\lambda g(x,s)}{1 + \lambda g(0,s)} \right]. \quad (10)$$

One can invert the Laplace transform to find the average bit corruption density as a function of x and t. Explicit forms are given in Ref. 12, for $d = 1$; the form is

$$\tilde{b}(x,t) = \langle \phi(x,t) \rangle = erf\left[\frac{|x|}{(2Dt)^{1/2}} \right] + \exp\left(\frac{\lambda |x|}{D} + \frac{\lambda^2 t}{2D} \right) \times erfc\left[\lambda \left(\frac{t}{(2D)} \right)^{1/2} + \frac{|x|}{(2Dt)^{1/2}} \right], \quad (11)$$

where $erf(z)$ and $erfc(z)$ are error functions [22]. Considering the asymptotic behavior of the above expression, for small x, we have

$$b(x,t) = b(0,t) + \left(\frac{2x^2}{\pi Dt} \right)^{1/2} + \cdots, x \ll (Dt)^{1/2}. \quad (12)$$

We find that the average bit corruption density at the origin ($x = 0$), $b(0,t)$, in Eq. (12) decays asymptotically as

$$b(0,t) = \left(\frac{2D}{\pi \lambda^2 t} \right)^{1/2} \left[l + O\left(\frac{D}{\lambda^2 t} \right) \right], \quad (13)$$

where $O\left(\frac{D}{\lambda^2 t} \right)$ represents the correction to the order of $\frac{D}{\lambda^2 t}$.

The above result reveals how the local spin temporally changes to reflect the local corrupting of the system mediated by the stochastic agent. This analytic result will be compared with the results obtained by the simulation. The intermediately large x behavior of $b(x,t)$ in Eq. (11) has two regimes:

$$b(x,t) = 1 - \left(\frac{2Dt}{\pi x^2} \right)^{1/2} \exp\left(\frac{-x^2}{2Dt} \right) + \cdots, (Dt)^{1/2} \ll x \ll \lambda t \quad (14)$$

and

$$b(x,t) = 1 - \left(\frac{\lambda t}{|x|} \right)^{1/2} \left(\frac{2Dt}{\pi x^2} \right) \exp\left(\frac{-x^2}{2Dt} \right) + \cdots, x \gg \lambda t. \quad (15)$$

To make the model closer to a real-world application, we assume the agents to be non-interactive; *i.e.*, they are unaware of each other's immediate presence. The nontrivial statistics stem from the fact that the disordering effects of the BAs statistically interact through the overlap of the BAs' histories. A single BA interferes with the previous disorder it has created; consequently, the corruption does not linearly increase in time. When many Brownian agents are introduced, each can disturb the corruption that another agent has created. As a result, the effect is more severe when many Brownian agents are present. The extension to many BAs is modeled within continuum theory. N independent Brownian Agents are introduced, and each can be described by position vector $R_\alpha(t)$, with $\alpha = 1, 2, \cdots, N$.

The equation of motion of the coarse-grained bit corruption density by N agents, $\phi^{(N)}(r,t)$, takes the form

$$\partial_t \phi^{(N)}(r,t) = -\lambda \phi^{(N)}(r,t) \sum_{\alpha=1}^{N} \Delta_l(r - R_\alpha(t)), \quad (16)$$

with the solution

$$\phi^{(N)}(r,t) = \Pi_\alpha^N \exp\left[- \lambda \int_0^t dt' \Delta_l(r - R_\alpha(t)) \right]. \quad (17)$$

On averaging over the path of the N agents, a particularly simple result of Eq. (16) is

$$b^{(N)}(r,t) = \langle \phi^{(N)}(r,t) \rangle = \left[b^{(l)}(r,t)^N \right]. \quad (18)$$

One can see that the local corruption density due to N agents is simply the Nth power of that due to one agent.

We now consider the probability distribution function, $P(b,x,t)$, of the local corrupted bit density. This function will provide information on the time evolution of the probability distribution that describes the local corruption behavior. Obviously, at very early time, the peak of the distribution is supposed to be in the vicinity of the origin. The complete analytic structure of $b(x,t;\lambda)$ is required to reconstruct the distribution function P. This suggests that by knowing the first moment of the corruption density, we can generate higher moments. Therefore, we can reconstruct the probability density function. We define P via

$$P(b,x,t) = \langle \delta(b - b_R(x,t)) \rangle, \quad (19)$$

where $b_R(x,t)$ is the stochastic field solution given in Eq. (13). We can express the δ function by using a frequency integral, and then we can expand it in powers of the field as follows:

$$\begin{aligned} P(b,x,t) &= \int_{-\infty}^{\infty} \frac{d\omega}{2\pi} e^{-i\omega b} \langle e^{i\omega b_R(x,t)} \rangle \\ &= \int_{-\infty}^{\infty} \frac{d\omega}{2\pi} e^{-i\omega b} \sum_{n=0}^{\infty} \frac{(i\omega)^n}{n!} \langle b_R(x,t)^n \rangle \\ &= \int_{-\infty}^{\infty} \frac{d\omega}{2\pi} e^{-i\omega b} \sum_{n=0}^{\infty} \frac{(i\omega)^n}{n!} \langle b(x,t;n\lambda) \rangle. \end{aligned} \quad (20)$$

We next take the Laplace transform of $b(x,t;n\lambda)$. From Eq. (10), we have

$$\begin{aligned} b(x,s;n\lambda) &= \frac{1}{s}\left[1 - \frac{n\lambda \hat{g}(x,s)}{1 + n\lambda \hat{g}(0,s)} \right] \\ &= \frac{g(0,s) - g(x,s)}{s g(0,s)} + \frac{g(x,s)}{s g(0,s)[1 + n\lambda g(0,s)]}. \end{aligned} \quad (21)$$

The first term is easily handled as it is independent of n. Thus, the sum over n for this yields a factor $e^{i\omega}$, which yields a factor $\delta(1-b)$ when integrated over ω. The second term is more interesting. For the details of how to perform the sum over n, we refer to Ref. 12. The final result for $\hat{P}(b,x,s)$ is

$$\begin{aligned} \hat{P}(b,x,s) &= \frac{g(0,s) - g(x,s)}{s g(0,s)} \delta(1-b) \\ &+ \frac{g(x,s)}{g(0,s)^2} \frac{1}{s\lambda b} \times \exp\left[-\frac{1}{\lambda g(0,s)} \ln\left(\frac{1}{b}\right) \right]. \end{aligned} \quad (22)$$

To this end, we need the explicit form for $\hat{g}(x,s)$ which is given by Eq. (9). Inserting this into Eq. (22) and inverting the Laplace transform, we have our final result:

$$\begin{aligned} P(b,x,t) &= \delta(1-b) erf\left[\frac{|x|}{(2Dt)^{1/2}} \right] + \frac{1}{(\pi t)^{1/2}} \frac{1}{\tilde{\lambda} b} \\ &\times \exp\{ -\left[\frac{|x|}{(2Dt)^{1/2}} - \frac{\ln b}{2\tilde{\lambda} t^{1/2}} \right]^2 \}, \end{aligned} \quad (23)$$

where $erf(z)$ is the error function [22] and $\tilde{\lambda} = \lambda/(2D)^{1/2}$. In particular, the probability distribution for the average bit corruption density at the origin takes the form

$$P(b,0,t) = \frac{1}{(\pi t)^{1/2}} \frac{1}{\tilde{\lambda} b} \times \exp\{ \left[-\frac{\ln(b)^2}{4\tilde{\lambda}^2 t} \right] \}, \quad (24)$$

which is a log-normal distribution.

If the asymptotic behavior of $b(0,t)$ is taken as $b(0,t) \sim \frac{1}{\sqrt{t}}$, $P(b,0,t)$ in Eq. (24) becomes

$$\begin{aligned} P(b,0,t) &= \frac{1}{\sqrt{\pi}\tilde{\lambda}} \times \exp\{ -\frac{1}{4\tilde{\lambda}^2 t} \left[\ln \frac{1}{\sqrt{t}} \right]^2 \} \\ &\times \exp\{ -\frac{(\ln t)^2}{t} \} = \exp\{ -\frac{1}{144t} - \frac{1}{6t^2} - \frac{3}{4t^3} \\ &+ \frac{26}{9t^4} + O\left(\frac{1}{t^5}\right) \} \times \exp\{ -\frac{1}{t} \} = \exp\{ -\left(\frac{1}{\sqrt{t}} \right)^2 \} \\ &= \exp\{ -b^2 \} \end{aligned} \quad (25)$$

which is the normal distribution, where $O\left(\frac{1}{t^5}\right)$ is the correction to order $\frac{1}{t^5}$. We now claim that the log-normal distribution approaches normality when t is infinitely large.

So far we have derived the local data bit corruption density and its probability distribution. In the next section, we shall focus mainly on the Monte Carlo simulation of $b(0,t)$ and its associated probability distribution $P(b,0,t)$ to explain our analytical finding. We then recap the analysis of the case of two dimensions [13]. Firstly, $b(0,t)$ was derived by using four different methods. One of them is the infinite-order perturbation theory of

$$\phi(\vec{r},t) = \exp\left[-\lambda \int_0^t dt' \Delta_l(\vec{r} - \vec{R}(t')) \right], \quad (26)$$

which was analyzed in Ref. 12 as Eq. (4) by using a Dirac delta function in place of a sink function $\Delta_l(\vec{r} - \vec{R}(t'))$. The sink function was used to avoid the difficulty of resumming the perturbation series. A short-time cut-off t_0 was introduced to regularize each term in the perturbation theory, which allowed one to extract the dominant contribution from each term in the perturbation expansion and then to resume the series. According to this method, $b(0,t)$ in two dimensions was found to be

$$b(0,t) = \frac{1}{1 + \tilde{\lambda} \log(t/t_0)}, \quad (27)$$

where $t_0 = \frac{2l^2 e^{-\kappa}}{D}$, ($\kappa = 0.57721\cdots$ is the Euler's constant) and $\tilde{\lambda} = \frac{\lambda}{2\pi D}$.

The calculation of the probability of the coarse-grained local bit corruption density at the origin $\phi(0,t)$ started

with the property $\langle\phi(0,t;\lambda)^n\rangle = \langle\phi(0,t;n\lambda)\rangle$ of the continuum theory in Eq. (26).

The known λ dependence of the first moment of $\phi(0,t)$ provided an easy way to reconstruct all the moments based on the above property and, thus, the probability density $P(\phi,0,t)$. The calculation of $P(\phi,0,t)$ is similar to one in one dimension with the accurate form of $\phi(0,t)$. If one considers $b(0,t)$ in Eq. (27) as $b(0,t) = \frac{1}{\tilde{\lambda}\log t}$ and uses it to calculate P, one obtains a distribution $P = \frac{b(0,t)}{\phi}$ which is singular at $\phi = 0$. Thus, the subleading correction to $b(0,t;\lambda)$ is very crucial to calculate the distribution correctly. The form of $b(0,t)$ in Eq. (32) in Ref. 13 is preferable for constructing P in that it contains the explicit form of $\omega(\tilde{\lambda})$. However, the complicated nature of ω makes the reconstruction of P hard to achieve.

Eq (32) in Ref. 13:

$$b(0,t) = \frac{1}{\omega(\tilde{\lambda}) + \tilde{\lambda}\log(t/\tau)} \tag{28}$$

coincides with Eq. (27) in the case of small λ giving $\omega(\tilde{\lambda}) \approx 1$ and the Laplace transform for $b(0,t)$:

$$\tilde{b}(0,s) = \frac{1}{s}\left[\frac{1}{1 - \tilde{\lambda}\log(\frac{s}{s_0})}\right]. \tag{29}$$

The reconstruction of P is possible from Eq. (27) and (29), and one finds

$$P(\phi,0,t) = \beta(t)\phi^{\beta(t)-1}, \tag{30}$$

where $\beta(t) = 1/\tilde{\lambda}\log(t/t_0)$. The probability distribution function in Eq. (30) is not singular at finite times and approaches the form $b(0,t)/\phi$ when $t \to \infty$.

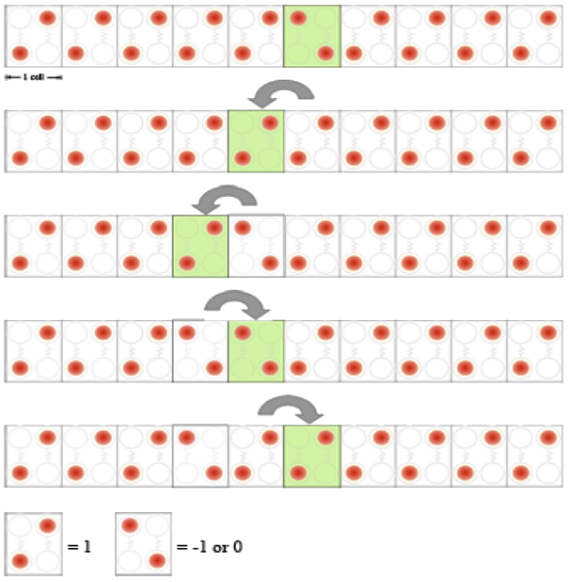

Fig. 2. Schematic of a system of juxtaposing cells in linear array (QCA wire). This can be used to represent a molecular or nano-bit array. Note that, typically, the electrons do not move from cell to cell, but each cell can "communicate" via a intercellular Coulomb interaction. By incorporating the stochastic corrupting agent(s), the state of the cell may be switched as the agent passes by. In other words, the polarization of the QCA cell can be oppositely induced by a stochastic agent, such as a quantum particle of heat or an electromagnetic wave.

IV. MONTE CARLO SIMULATION RESULTS

Our aim in this section is to show the validity of our theoretical results obtained in the previous section. To do so, we have performed Monte Carlo simulations of the discrete model defined in Section III. All results are obtained for a one-dimensional ($d = 1$) chain and a two-dimensional ($d = 2$) square lattice of binary bits which at each site can take either the value 1 (spin up) or -1 (spin down). The system size is considered negligible so long as one ensures that the BA never touches the boundaries in any of its realizations up to the latest time at which data are extracted. Thus, the system is infinitely large. We performed an average of over 10^6 realizations (or runs) with each run starting with the same initial configuration; namely, all spins are pointed up except the spin of the starting point of the BAs, which is set to be -1 (down) in order that immediately after all the BAs have moved away, the spin at the starting point has value $= 1$ as shown in Fig. 3, the illustration in one dimension. Then, N random walk agents are introduced to the starting point (origin). At each Monte Carlo step, all N agents randomly walk to either one of its $2d$ neighboring sites and flip the spin of visited site before leaving.

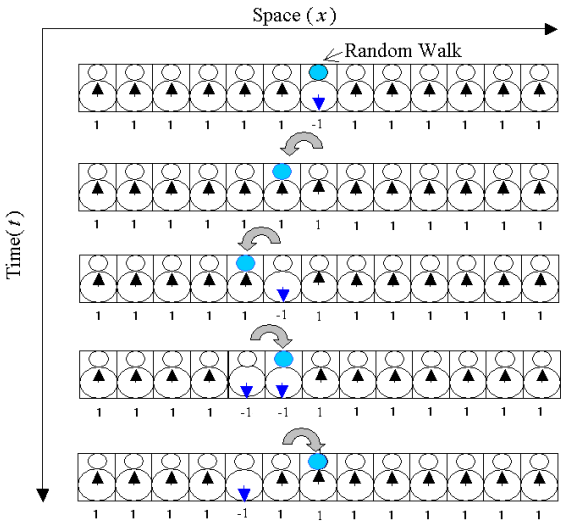

Fig. 3. Illustration of the data corruption processes for dimension $(d) = 1$, hopping rate of $(p) = 1$, and flipping rate of $(q) = 1$. The initial uncorrupted state is shown on the second row, with the BA being represented by a filled circle. From the top, we show a typical walk of 4 steps. The BA switches a bit each visit, so those bits visited for an even number of times are restored to their original values.

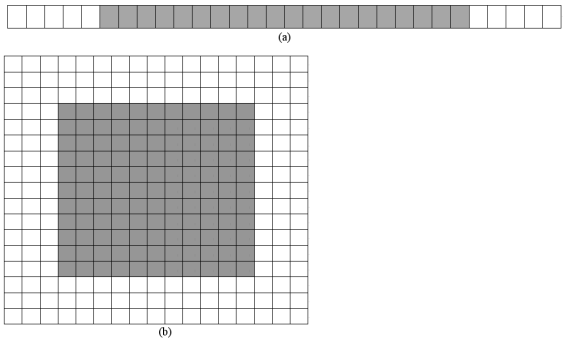

Fig. 4. Illustration of a patch (shaded region) in (a) a one-dimensional infinite system and (b) two-dimensional infinite system representing the origin. The starting points of the agents are at the boundary of the patch.

We let the BAs corrupt the system independently with the consequence that multiple occupancies are allowed. We focused on the local corruption at the origin, so we measured the average bit corruption density at the origin denoted by $b(0,t)$, where the BAs started corrupting the system. As mentioned, it makes no sense to measure moments of individual spins at the origin because an odd visit at the origin by a BA gives -1 while an even visit yields unity. As a result, the distribution for the average bit corruption density at the origin is not consistent with the analytic results obtained by using continuum theory. Therefore we defined a coarse-grained bit corruption over a patch containing 20 spins for one dimension, Fig. 4(a), and over a patch containing 121 spins for two dimensions (perviously used in Ref. 13), Fig. 4(b), representing the bit at the origin to produce some results that can be compared to theoretical ones. The patch size consideration in two dimensions will be stated in Section IV. The patch size is chosen arbitrarily as a compromise between computational performance and a realistic time scale and length scale for the dynamics. In fact, we have varied the patch size and found a patch of 20 bits is somehow the optimal one. In addition, the agents are initially allocated evenly on both ends of the patch to avoid internal decimation by the transient motion of the agent. We investigated and obtained many meaningful results and new simulation strategies.

1. One Dimensional

A. Time-regime Observation

In Fig. 5, over the same patch size of 20 due to 5 BAs, the origin is corrupted more often by one or more walkers. It also becomes more difficult to obtain data for time spanning more than one decade. One arrives at a compromise between the patch size and the number of walkers to obtain a longer span in each time regime byrealizing that in order for a BA to wander twice the distance, it will take 4 times as long to reach the distance

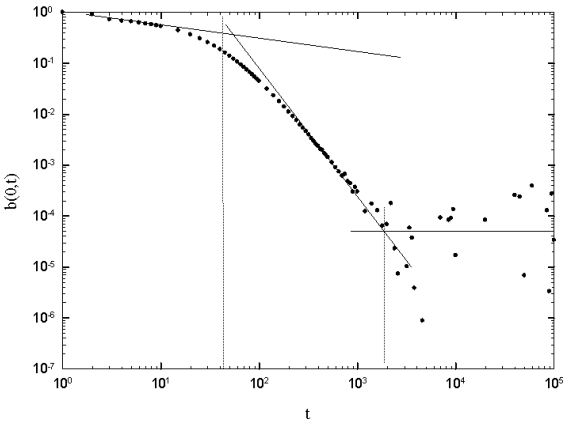

Fig. 5. Log-log plot of the average bit corruption density at the origin $b(0,t)$ versus time for $d = 1$, $p = 1$, and $q = 1$ due to 5 BAs. The approximate crossover times from regime I to regime II and from regime II to regime III are shown, respectively, on the t axis at the intersections of the straight lines.

[23]. Nevertheless, in Fig. 5, we can see a crossover from a scaling regime when $t = 10^3$; the values of $b(0,t)$ are very close to zero with high fluctuations. A typical plot of the time evolution of the average bit corruption density will have three regions separated by two crossover times.

Now, we will consider the long time spatial behavior for small x (a site close to the origin). From Eq. (12) we have $\lim_{t\to\infty} b(x,t) = \lim_{t\to\infty} b(0,t) = 0$ when $x = (Dt)^{1/2}$. These time limits imply that the BA always corrupts the bits in small region around the origin in an oscillatory manner, forward and backward, instead of moving away in a forward direction. Moreover, the BA will never visit sites x further than $(Dt)^{1/2}$ from the origin. This is proven by $\lim_{t\to\infty} b(x,t) = 1$ when $x = (Dt)^{1/2}$.

B. A Compromise on the Patch Size

The results in Fig. 6 show simulations of the time evolution of the bit corruption density at the origin $b(0,t)$ for different patch sizes. Eq. (13) predicts that $b(0,t)$ will decay as $1/\sqrt{t} = t^{-0.5}$ when t is not infinitely large. If logarithmic scales are used, the power law dependence is seen as a straight line. From the simulated results in Fig. 6 at early time, there is no simple scaling form for $b(0,t)$ for any patch size. The small-time behavior of the random walk is transient in the early time regime (regime I). This regime can be seen to be less than a decade in t. When $t = 10^2$, the average bit corruption density at the origin $b(0,t)$ over a patch size of 20 decays as $t^{-0.4936}$. The exponent calculated in the last two decades of the log-log plot (for the optimal fit) leads to the theoretical scaling $b(0,t) \sim t^{-0.5}$. All further simulations will be done for a patch of 20 bits. Therefore, the patch size should be taken into account to gain higher quality re-

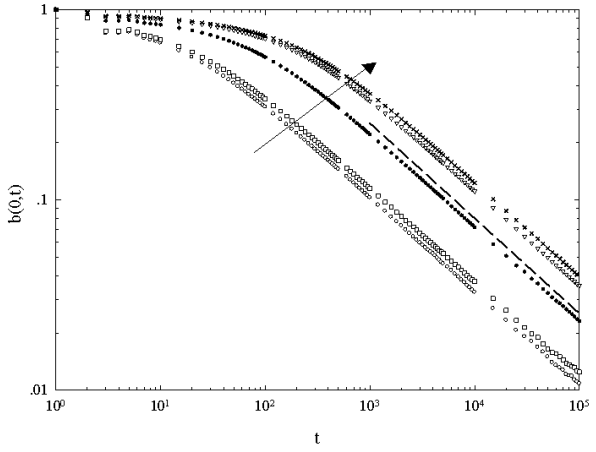

Fig. 6. Log-log plot of the average bit corruption density at the origin $b(0,t)$ versus time for a patch size of 10, 11, 20, 30, and 33 for $d = 1$, $p = 1$ and $q = 1$ due to 1 BA. The arrow shows the increment of the patch size.

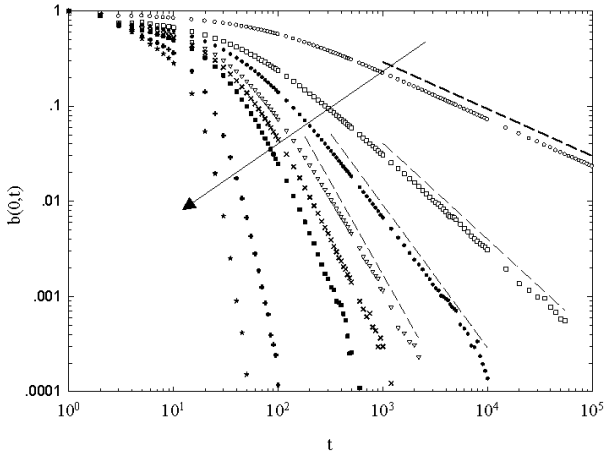

Fig. 7. Log-log plot of the local bit corruption density at the origin $b(0,t)$ versus tim for $d = 1$, $p = 1$, and $q = 1$ due to 1, 2, 3, 4, 5, 6, 16, and 32 BAs. The arrow shows the increment in the number of BAs. The dashed lines have slopes of -0.4992, -1.0104, -1.4999 and -1.9487, respectively, along the direction of the arrow and show the range of time over which the exponent is extracted.

sults because it affects the time scale for a random walk to wander from patch to patch. The time regime in which the power law is extracted is the so called scaling regime or intermediate time regime (regime II). $b(0,t)$ crosses over from the transient regime to the scaling one at the crossover time. The long time behavior of Eq. (13) is $\lim_{t\to\infty} b(0,t) = 0$. This shows the infinitely-long-time regime (regime III). Because of the considerably large time consumption and the trivial dynamic, we have not made infinitely long runs in regime III.

C. The Corruption Process Due to N Independent Agents

We have extensively investigated the cases of more BAs. The results are shown in Fig. 7. We present $b(0,t)$ from the early time regime to the scaling regime to show the stepping over and to verify Eq. (18). From Eq. (18) the average bit corruption density by two agents is given by $[b^{(1)}(0,t)]^2 = [b(0,t)] \sim [t^{-0.5}]^2 = t^{-1}$. We reconsider $b^{(N)}(0,t)$ in Eq. (21) as $b^{(N)}(0,t) \sim t^{\gamma}$.

The numerical values of γ due to the results shown in Fig. 7 are presented in Table 1 along with the results from our computer simulations.

A higher power law decay of $b(0,t)$ with two agents is found from Fig. 7, $b(0,t)$ decays more rapidly ($t^{1.0104}$) than it does for a single agent. Since the BAs starting from the same origin are independent, the spreading of the 2 BAs is symmetrical about the origin, and the mean position of BAs does not change from step to step, but remains 0 [6]. The BAs always return to the origin [23]. As a result, the origin is corrupted more frequently, and the early-time and scaling regimes are shorter when we have more agents. The average number of distinct sites N BAs have visited at time t is $\sqrt{t \ln N}$, where N is large [24]. The entire span of N BAs still appears in the factor $\sqrt{t}$. They corrupt a bit within the finitely bounded region. So far, in the cases of 3 and 4 BAs, the scaling forms extracted from the simulation results are $b^{(3)}(0,t) \sim t^{1.4999}$ and $b^{(4)}(0,t) \sim t^{-1.9487}$, respectively, which are in good agreement with the theoretical results. The conventional scaling in Eq. (18) holds. The scaling regime in case of more than 4 BAs is less than one decade in t. To extract the scaling, we have to enlarge the patch size and run the simulation for a long enough time to gain a longer span of data in the scaling regime. The probability that the origin has been visited by at least one of the N BAs is 1 when N is enormously large [24]. This indicates that the origin is strongly corrupted when many agents are introduced to the system.

Table 1. Predicted values of γ compared with simulated values. The numbers in parentheses are the values of R^2 from the linear regression fitting data in Fig. 7.

N	γ_{theory}	$\gamma_{simulation}$
1	-0.5	-0.4936 (1.0000)
2	-1.0	-1.0104 (0.9992)
3	-1.5	-1.4999 (0.9952)
4	-2.0	-1.9487 (0.9977)

D. The Probability Distribution for $b(0,t)$

The results in Fig. 8 (a)-(d) are given to show the probability distribution of all possible values of $b(0,t)$ due to one and more uncorrelated BAs. To find the possible asymmetry of the probability distribution function around the mean, we considered the first index of the

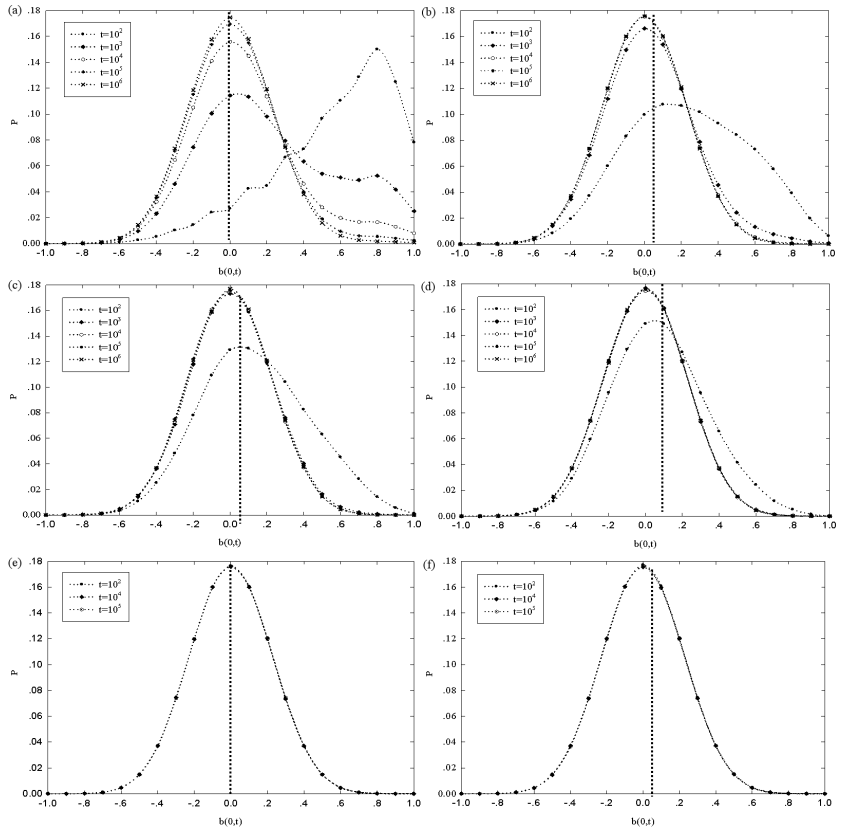

Fig. 8. Simulated probability distribution for the average bit corruption density at the origin, $b(0,t)$ for $d = 1$, $p = 1$, and $q = 1$ due to (a) 1, (b) 2, (c) 3, (d) 4, (e) 16, and (f) 32 BAs starting at the boundary of the patch.

shape, called the "skewness coefficient" which is defined as the standardized third central moment [25]. The skewness coefficient of a normally distributed random variable b is $\alpha_3(b) = \mu_3/(\sqrt{\mu_2})^3$, where μ_2 and μ_3 are the second and the third central moments of b, respectively. If the distribution is symmetric around the mean, then $\alpha_3 = 0$; the converse is not true.

We reproduced the data with a single BA as shown in Fig. 8(a). In the early time regime when $t = 10^2$, the simulated probability distribution for $b(0,t)$ due to one agent is log-normal (Eq. (24)). The distribution curve has a robust tail for values of average bit corruption density close to unity; *i.e.*, for $b(0,t) = 0.8$, most of the time only 2 bits in the patch are corrupted. The fact that BA on a one-dimensional lattice always returns to the origin [26] is critical for this event. Surprisingly, at a large time $t = 10^5$, the distribution has completely changed from log-normal to normal. The peak occurs when $b(0,t) = 0$ with probability 0.1675. The distribution is also normal at a larger time of $t = 10^6$ with the peak taking place at $b(0,t) = 0$ with probability 0.1746. An important feature of this distribution unambiguously points out that realizations where the spins at the origin will be half corrupted and half uncorrupted will have the highest probability of occurrence.

In the case of two BAs with one BA at each edge of the patch, in the distribution for $b(0,t)$ at $t = 10^2$, the peak is shifted to the left to $b(0,t) = 0.1$, very close to 0, and the robustness disappears. Also, we mostly find that 9 out of 20 bits are corrupted. Not as expected, the origin is more strongly corrupted, and the overlap of the path of the individual agent should be appropriate for a description of this event. All distributions at $t \geq 10^4$ become normal and coincide. For 3 and 4 BAs, the distributions for $b(0,t)$ approach normality earlier than they do for 1 and 2 BAs with the same features. The shapes of the distribution at the last three times look very symmetric and have a skewness coefficient very close to 0.

In Fig. 8 (e) and (f) with larger number of BAs, we see that the probability distribution for $b(0,t)$ approaches normality at smaller times, obviously faster than it does for the case of a small number of BAs. It is clearly seen that as more agents are considered, the faster the distribution function will approach normality. This reflects the high fluctuation of the BAs. Another way to put it is that the BAs wander within the space of an approximate length of $\sqrt{t \ln N}$ from the origin. To distinguish two symmetric distributions with respect to their peaks and tails, we consider another shape index called the "Kurtosis coefficient" which is defined as $\alpha_4(b) = \mu_4/(\mu_2)^2$, where μ_4 is the fourth central moment of b. The nor-

mal distribution $f(x;\theta) = \frac{1}{\sigma\sqrt{2\pi}}\exp[\frac{-(x-\mu)^2}{2\sigma^2}]$, where $\theta := (\mu, \sigma^2) \in \Re \times \Re_+$, and $x \in \Re$ has $\mu_4 = 3$. The 16 and 32-BA probability distributions at all times have common Kurtosis coefficients of $\mu_4 \sim 2.9$ which means that they have the same peak (mean values) relative to the shapes of the tails and that their peaks are slightly flatter than normal. The peaks of all normal distributions are at $b(0,t) = 0$ with the probability bounded from above at 0.18. The essential features of the asymptotic distribution are independent of time and the number of the Brownian agents. In all cases, for large time, the observed probability of having the origin completely corrupted or uncorrupted-the probability that all spins of the origin are pointed down or up- is extremely close to 0. This agrees with the heuristic expressions in Eqs. (4) and (5). This is in good agreement with the fact that the average bit corruption density at the origin decays asymptotically as predicted by Eq. (13).

2. Two Dimensional

A. The Patch Size Effect on the Simulation Results

In Eq. (27), due to one BA, $b^{(1)} = 1/[1 + \tilde{\lambda}\log(t/t_0)] \sim 1/[A + \tilde{\lambda}\log t \sim C_1^{'}/\log t]$. On the other hand, $1/b^{(1)} \sim C_1 \log t$, so the plot of $1/b^{(1)}$ against $\log t$ gives a straight line. We have tried measuring $b(0,t)$ due to one agent at the origin (single site) and on different patches of 9, 25, 49, 81, and 121 bits. In Fig. 9, we investigate the effect of the patch size and find different values of constant C_1 in the above equation. Presumably the patch size affects only the prefactor C_1. The patch size has no significant effect on the logarithmic time dependence of $b(0,t)$. We then choose the patch of 121 bits to simulate $b(0,t)$, which was considered to be practical for the measurement of the probability distribution for $b(0,t)$ we looked forward to.

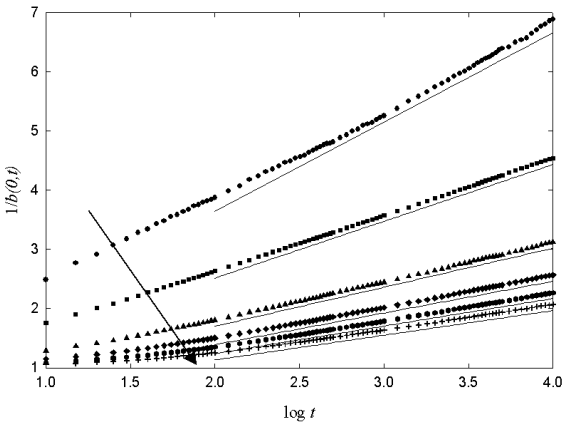

Fig. 9. Plot of $1/b(0,t)$ due to 1 BA versus $\log t$ over a square patches of 1, 9, 25, 49, 81, and 121 bits for $d = 2$, $p = 1$, and $q = 1$. The arrow shows the increment of patch size. The thick straight lines have slopes of 1.507, 0.9585, 0.6590, 0.5335, 0.4652, and 0.417 , respectively, (from top to bottom).

B. The Logarithmic Time Dependence of $b(0,t)$

To approach the practical application closer, we performed two-dimensional simulations similar to the one-dimensional ones; we measured the bit corruption density at the origin represented by square patch of 121 bits, $b(0,t)$, due to 1 to 4 BAs. In the case of one agent, the plot of $1/b^{(1)}$ against $\log t$ gives a straight line, as shown in Fig. 10(a). We know from Eq. (18) that $b^{(N)} = [b^{(1)}]^N$ in the case of 2 BAs, so we find that $b^{(2)} \sim (C_1)^2(\log t)^2$ or $1/b^{(2)} \sim C_2(\log t)^2$. This is verified by a plot of $1/b^{(2)}$ versus $(\log t)^2$, which can be fitted by a straight line. Inductively, we have $1/b^{(N)} \sim C_N(\log t)^N$, where the $C_i, i = 1, \cdots, N$, are constants. The plot of $\log[1/b^{(N)}]$ against $\log[(\log t)^N]$ in Fig. 10(e) for infinitely large times has the same slope for any number N of independent agents.

With more BAs lined up on the boundary of the patch, the decay of $1/b(0,t)$ is shown again in Fig. 10(c) and 10(d) to be proportional to the Nth power of $logt$. The local bit corruption density at the origin, $b(0,t)$, in one and two dimensions have a common N dependence but in different manner. The decay in one dimension, $b^{(N)}(0,t) \sim (\sqrt{t})^N$, is drastically higher than two dimensions, $b^{(N)}(0,t) \sim (\log t)^N$, due to fewer paths of the BAs returning to the origin [24].

C. Probability Distribution for $b(0,t)$ due to N Independent Agents

The probability distribution for $b(0,t)$ due to one BA in Fig. 11(a) agrees with the results in Ref. 13, which show three behavior sets by a crossover time $\beta(t^*) = 1$. At small $t \ll t^*$, the distribution has the most weight near $b = 1$. Then, for intermediate $t \sim t^*$, $b(0,t)$ is uniformly distributed over the entire interval of b. For large $t \gg t^*$, the distribution curve is positively skewed and approaches the form $1/b(0,t)$. This crossover disappears from the case of multiple BAs in Fig. 11(b)-(f). From early to late time, the skewness of the distribution curve changes from negative to positive, and the skewness coefficient decreases when the more BAs are introduced. At large time with 16 BAs and all time with 32 BAs the distribution curves are symmetric (the Skewness coefficients are very close to 0) about the mean $b(0,t) = 0$ and have the common Kurtosis coefficients $\alpha_4 \in [2.95, 3.01]$ very close to 3. This implies that they have about the same peak and tail shapes.

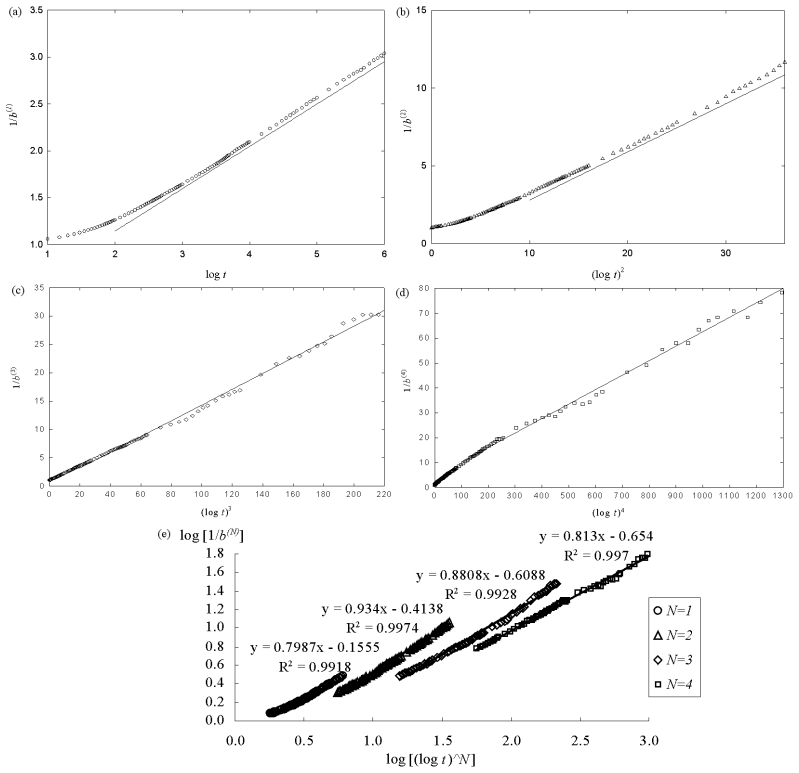

Fig. 10. (a)-(d) are plots of $1/b^{(N)}$ versus $(\log t)^N$ due to $N = 1$, 2, 3, and 4 BAs, respectively, and (e) is a plot of $\log[1/b^{(N)}]$ versus $\log[(\log t)^N]$ for $N = 1$, 2, 3, and 4; $d = 2$, $p = 1$, and $q = 1$.

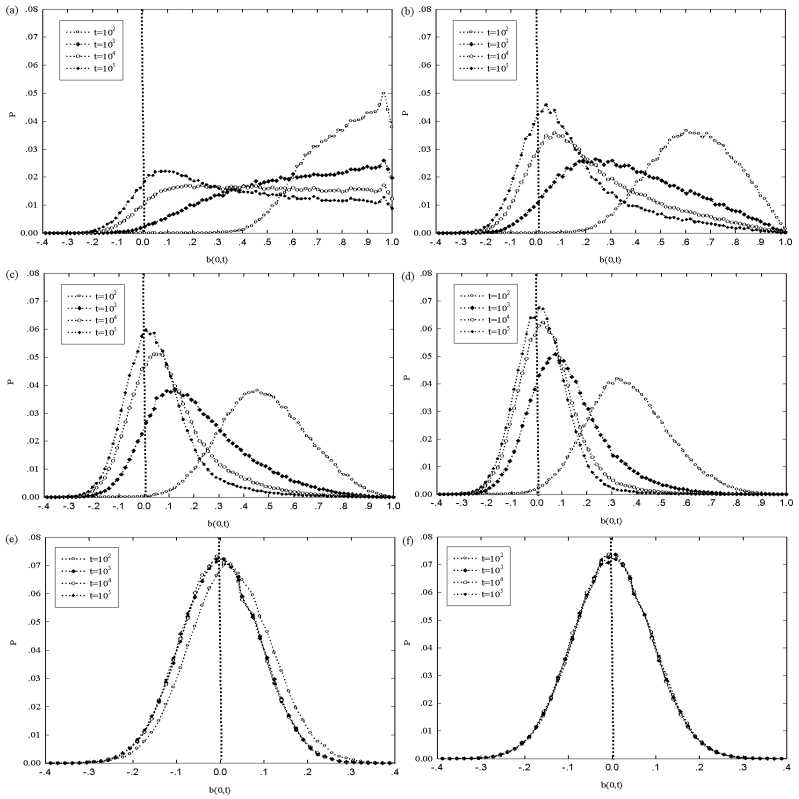

Fig. 11. Simulated probability distribution for the average bit corruption density at the origin, $b(0, t)$ for $d = 2$, $p = 1$, and $q = 1$ due to (a) 1, (b) 2, (c) 3, (d) 4, (e) 16, and (f) 32 BAs starting at the boundary of the patch.

V. SUMMARY AND CONCLUSION

We have introduced and solved a model in which BAs interact with a binary nano-bit system. We have focused on the local corruption at the origin where the BAs start. We have performed computer simulations to calculate $b(0,t)$ for different patch sizes, which is regarded as a continuous approach. We found that a patch of 20 bits gave the optimal result for the scaling behavior of $b(0,t)$ with regard to the computation run time and the patch size. In the simulation results, the power law scaling in the scaling regime due to 1 – 4 BAs obeys the relation $b^{(N)}(r,t) = [b^{(1)}(r,t)]^N$- in good agreement with the predictions of the continuum model. In brief, $b(0,t)$ depends sensitively on the number of BAs in terms of the overlap of the paths of different walkers and how often the BAs visit the patch [24]. In order to see the time evolution of $b(0,t)$ when there are more than 4 BAs in this regime and to extract the power law scaling over more than one decade, one has to compromise between the size of patch and the number of BAs. The decay of $b(0,t)$ due to BAs is not linearly proportional to $b(0,t)$ due to 1 BA, but instead it goes as the Nth power of $b(0,t)$. The origin is strongly corrupted by multiple BAs because all of the independent BAs always return to the origin and corrupt its spin. N agents which are non-interacting will interfere strongly with each other; in other words, their histories overlap. When time is infinitely large, $b(0,t)$ approaches 0, which implies a 50 % chance of finding the site to be spin up or down. This agrees with the time limit of $b(0,t)$. The fluctuation at this equilibrium is relatively large compared to that in the scaling regime.

We then investigated how often all possible values of the corruption at the origin occur. This was found by looking at the probability distribution for $b(0,t)$ at particular times. For the case of 1 BA, in the early time regime, the distribution is log-normal with a robust tail at a value near 1. This reveals an extreme fluctuation at the origin and a high probability that the origin will only be slightly corrupted. The distribution approaches normality as time proceeds, with the highest probability occurring at $b(0,t) = 0$. This means that the origin is steadily corrupted. The distribution approaches a normal distribution quicker when there is more than one BA. In the long-time limit, $P(b,0,t)$ converges to a normal distribution. The peak of the normal distributions remains at the same place, at $b(0,t) = 0$. In contrast to $b(0,t)$, the characteristics of the normal distributions are independent of N and time.

In two dimensions, we found that the patch size affected only the prefactor of the time evolution of $b(0,t)$, not its feature. The average bit corruption at the origin due to agents decayed as the inverse of the Nth power of $\log t$, which is slower than that in one dimension due to the boarder region the BAs can wander through and to the BAs returning to the origin less often [24]. This affects the shape of the probability distribution curves. For the same number of BAs, the time evolution of the distribution in two dimensions approaches normality slower than it does in one dimension. The investigation and the conclusion in our study provide insight into one specific example of stochastic binary nano-bit corruption mediated by a random or Brownian agent. They should be helpful to future researchers who wish to study data corruption for the purpose of increasing the reliability or stability of a nanodevice.

The application of the models is wide open. There are many directions for further work; foremost among them are

1. calculating other local and global parameter densities,
2. calculating the correlation function or the structure factor,
3. investigating the universality of the corruption process, and
4. studying the case of biased agents and other generalized couplings

to make a stronger connection to practical processes or to real-world applications on soft-error reduction.

Finally, we want to remark that this work is at least an extensive investigation of noise or fluctuations caused by a Gaussian fluctuator and non-equilibrium statistical mechanics in nano-electronic systems. This study of "statistical-mechanical electronics" spans two disciplines, statistical physics and molecular electronics system, and leads to a general picture that bridges these two disciplines. We believe and hope that our work has scientific, engineering, and computer implications. Scientifically, this work is an extensive study of non-equilibrium statistical mechanics via a stochastic process in the context of a molecular bit or nano-bit system, which will make several significant contributions to the understanding of noise processes in nano-electronic devices. The technological importance is a demonstration of how the fundamental physical considerations evolve to practical high-performance novel electronic designs.

ACKNOWLEDGMENTS

We would like to thank Prof. J. Poulter, Prof. Y. Lenbury, Prof. I. M. Tang, Dr. M. Chuedoung, and Ankana Boondirek for their helpful comments and suggestions. This research is supported in part by a scholarship under the Staff Development Project of the Commission on Higher Education from Naresuan University, Thailand. The grant from Institute of Science and Technology for Research and Development, Mahidol University, Thailand and the Thailand Research Fund through grant numbers MRG4880161 and RTA4580005 are also acknowledged.

REFERENCES

[1] M. L. Roukes and S. Fritz, *Understanding Nanotechnology* (Warner Books, 2002).
[2] K. Bogunia-Kubik and M. Sugisaka, BioSystem **65**, 123 (1991).
[3] K. E. Drexler, *Engines of Creation: The Coming Era of Nanotechnology* (Anchor Books, New York, 1986).
[4] R. A. Freitas, Nanomedicine, Vol. I *Basic Capabilities* (Landes Bioscience, Texas, 1999).
[5] G. M. Whiteside, Nature Biotechnology **21**, 1161 (2003).
[6] H. C. Berg, *Random Walks in Biology*, expanded edition (Princeton University Press, New Jersey, 1993).
[7] D. R. Koenig, D. V. Scheible and R. H. Blick, Appl. Phys. Lett. **85**, 157 (2004).
[8] T. A. Fulto and G. J. Doland, Phys. Rev. Lett. **59**, 109 (1987).
[9] H. Grabert and M. H. Devoret, *Single Charge Tunneling* (Plenum, New York, 1992).
[10] R. H. Chen, A. N. Korotkov and K. K. Likharev, Appl. Phys. Lett. **68**, 1954 (1996).
[11] V. A. Froltsov, A. G. Mal'shukov and K. A. Chao, Phys. Rev. B **64**, 073309 (2001).
[12] T. J. Newman and W. Triampo, Phys. Rev. E **59**, 5172 (1999).
[13] W. Triampo and T. J. Newman, Phys. Rev. E **60**, 1450 (1999).
[14] *The 1997 National Technology Roadmap for Semiconductors* (SEMATECH, Austin, TX, 1997).
[15] M. C. Petty, M. R. Bryce and D. Bloor, *Introduction to Molecular Electronics* (Oxford University Press, New York, 1995).
[16] C. P. Collier, E. W. Wong, M. Belohrad, F. M. Raymo, R. F. Stoddart, P. J. Kuekes, R. S. Williams and J. R. Helth, Science **285**, 391 (1999).
[17] J. Chen, M. A. Reed, A. M. Rawlett and J. M. Tour, Science **286**, 1550 (1999).
[18] C. S. Lent, P. D. Tougaw, W. Porod and G. H. Bernstein, Nanotechnology **4**, 49 (1993).
[19] C. S. Lent, Science **288**, 1597 (2000).
[20] A. O. Orlov, R. Kummamru, R. Ramasubramanian, C. S. Lent, G. H. Bernstein and G. L. Snider, J. Nanosci. Nanotechnol. **2**, 351 (2002).
[21] C. S. Lent, B. Isaksen and M. Lieberman, J. Am. Chem. Soc. **125**, 1056 (2003).
[22] M. Abramowitz and I. A. Stegun, *Handbook of Mathematical Functions*, 10th edition (Dover, New York, 1972).
[23] R. Czech and K. W. Kehr, Phys. Rev. E **53**, 1783 (1984).
[24] H. Larralde, P. Trunfio, S. Haylin, H. E. Stanley and G. H.Weiss, Phys. Rev. A **45**, 7128 (1992).
[25] S. Aris, *Probability Theory and Statistical Inference Econometric Modeling with Observational Data* (Cambridge University Press, Cambridge, 1998).
[26] S. R. Finch, *Mathematical Constants* (Cambridge University Press, New York, 2003).